Chemical Engineering Communications

ISSN: 0098-6445 (Print) 1563-5201 (Online) Journal homepage: https://www.tandfonline.com/loi/gcec20

Enhancement of biogas production via green ZnO nanoparticles: experimental results of selected herbaceous crops

Mohamed A. Hassaan, Antonio Pantaleo, Luigi Tedone, Marwa R. Elkatory, Rehab M. Ali, Ahmed El Nemr & Giuseppe De Mastro

To cite this article: Mohamed A. Hassaan, Antonio Pantaleo, Luigi Tedone, Marwa R. Elkatory, Rehab M. Ali, Ahmed El Nemr & Giuseppe De Mastro (2021) Enhancement of biogas production via green ZnO nanoparticles: experimental results of selected herbaceous crops, Chemical Engineering Communications, 208:2, 242-255, DOI: 10.1080/00986445.2019.1705797

To link to this article: https://doi.org/10.1080/00986445.2019.1705797

Published online: 26 Dec 2019.

CHEMICAL ENGINEERING COMMUNICATIONS
2021, VOL. 208, NO. 2, 242–255
https://doi.org/10.1080/00986445.2019.1705797

Enhancement of biogas production via green ZnO nanoparticles: experimental results of selected herbaceous crops

Mohamed A. Hassaan[a,b], Antonio Pantaleo[b], Luigi Tedone[b], Marwa R. Elkatory[c], Rehab M. Ali[d], Ahmed El Nemr[a], and Giuseppe De Mastro[b]

[a]Marine Pollution Lab, National Institute of Oceanography and Fisheries, Alexandria, Egypt; [b]Agriculture and Environmental Sciences Department, Bari University, Bari, Italia; [c]Advanced Technology and New Materials Research Institute (ATNMRI), City for Scientific Research and Technological Applications (SRTA-City), Alexandria, Egypt; [d]Fabrication Technology Department, Advanced Technology and New Materials and Research Institute (ATNMRI), City of Scientific Research and Technological Applications (SRTA-City), Alexandria, Egypt

ABSTRACT
The key to bio-gasification is the lignocellulosic materials provided in the herbaceous crops which are considered to be renewable energy resources. This study focuses on pretreatments of five selected biomass (barley, durum wheat, Abyssinian cabbage, rapeseed, and triticale) to be utilized for biogas production using chemical and green ZnO nanoparticles which were synthesized from durum wheat extract. The experimental tests were carried out to compare the different anaerobic digestion (AD) conversion efficiency with and without ZnO nanoparticles treatment on the biogas production yield. The total solids (TS), volatile solids (VS), ash content, carbon (C), hydrogen (H), and nitrogen (N) content of the tested biomass have been measured. The results revealed that durum wheat has the highest biogas yield of 353 mL/g VS compared with control biomass which produced only 271 mL/g VS. The highest specific biogas production was attained when the durum wheat was treated with 10 mg/L of chemical and green ZnO nanoparticles which produced 422 mL/g VS and 457 mL/g VS respectively compared with the control that produced only 353 mL/g VS. All results have a significant level of $p < 0.05$.

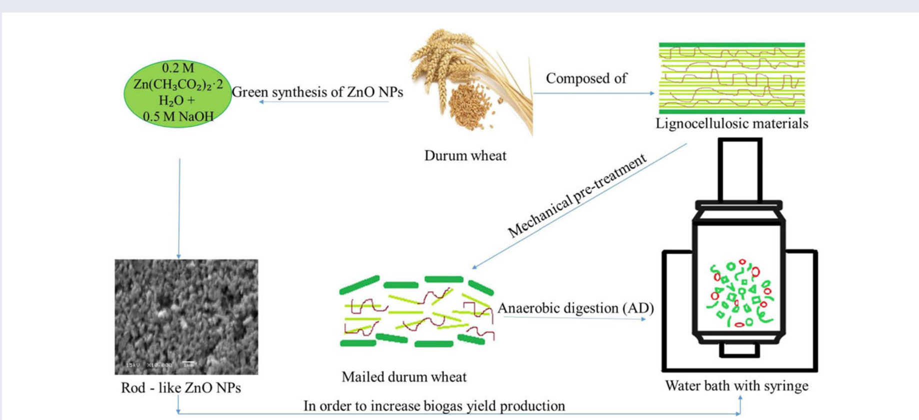

Schematic diagram of the biogas production from durum wheat.

KEYWORDS
Abyssinian cabbage; barley; biogas production; durum wheat; field crops; rapeseed; triticale; ZnO nanoparticles

Introduction

Anaerobic digestion for biogas/bio-methane production is a reliable and widely implemented technology to produce clean renewable energy that achieves multiple environmental benefits. Switching from fossil fuels to biogas generally decreases the emissions not only of greenhouse gases but also of hydrocarbons, sulfur oxides, and

CONTACT Mohamed A. Hassaan ma.hassaan@niof.sci.eg; mhss95@mail.com Marine Pollution Lab, National Institute of Oceanography and Fisheries, Alexandria 21556, Egypt.
Color versions of one or more of the figures in the article can be found online at www.tandfonline.com/gcec.

nitrogen (Borjesson and Berglund 2006). Furthermore, biogas has the advantage of lower nitrogen oxides emissions on respect to other biomass fuels, such as biodiesel (Kamel et al. 2018).

The existence of trace metals is crucial for the enzymes' activity in the methanogenic systems. The addition of trace metals to anaerobic digesters leads to the acceleration and stabilization of the biogas production performance (Qiang et al. 2012; Takashima et al. 2009). Some previous experiments have been conducted to control the requirements and optimize the trace elements concentration. They revealed that the deficiency of elements, such as Ni or Co, caused impaired substrate conversion to methane, volatile fatty acids (VFA) accumulation, and digester acidification and breakdown (Schmidt et al. 2013).

Gustavsson et al. (2011) stated the necessity to augment trace elements for a steady process in wheat silage fed mesophilic biogas production at a higher organic loading rate of 4 g VS L^{-1} day^{-1} with dosages of 0.5 g Fe, 0.5 mg Co, and 0.2 mg Ni L^{-1} day^{-1}. The presence of heavy metal ions throughout anaerobic degradation of organic matter is recognized to be essential for various reactions. Moreover, in other cases, the digester functioning was improved simply by adding trace elements and thus enhancing methanogenic activity. However, higher concentrations of these elements can prevent biodegradation processes in the anaerobic reactors.

Several studies investigated the use of different types of nanoparticles (NPs) to enhance biogas production and improve anaerobic digestion. Few studies investigated the effect of ZnO NPs, among them Mu et al. who examined four chemically synthesized metal oxides; ZnO, TiO_2, SiO_2, and Al_2O_3 NPs and stated that only chemical ZnO NPs have inhibitory influences on methane production. Lowering ZnO NPs dose than (6 mg/g TS) has no impact on the methane production (Abdelsalam et al. 2017; Amirante et al. 2018; Mu et al. 2011; Risco et al. 2011).

Abdelsalam et al. verified that NPs can enhance the anaerobic process and stimulate the slurry digestion, which improves the biogas and methane generation. The impacts of NPs on biogas and methane generation were examined using a specially constructed batch anaerobic reactor. For this reason, a series of 2 L biodigesters were created and employed to study the impacts of the Fe NPs and Fe_3O_4 NPs with different concentrations on biogas and methane generation. The aforementioned NPs delivered higher biogas and methane yields than their salt ($FeCl_3$) and the control. Additionally, the dose of 20 mg L^{-1} Fe_3O_4 and 20 mg L^{-1} Fe NPs magnetic NPs considerably raises the biogas volume by 1.66 and 1.45 times than the biogas volume formed by the control, respectively. Furthermore, the methane volume has been improved by 1.96 and 1.59 times than the methane volume formed by the control, respectively. However, to the best of author's knowledge, this is the first research that describes and compares the impact of green and chemical ZnO NPs utilization with different concentrations on biogas production from durum wheat. The content of innovation of the proposed research is to evaluate five herbaceous crops (barley, durum wheat, Abyssinian cabbage, rapeseed, and triticale) for biogas production and compare their performance to select the most effective one. On the other hand, highly pure crystalline ZnO NPs were synthesized with new morphologies using two different routes; green synthesis using the extract of a certain crop (durum wheat) and chemical synthesis to investigate their effects on the biogas production yield and the process timing.

Materials and methods

A flow chart of the experimental tests with the proposed procedure steps is shown in Figure 1.

Substrates

The substrates which used for this work are biomass obtained from five field crops (barley, durum wheat, Abyssinian cabbage, rapeseed, and triticale). Inoculum is a digested liquid product for the biogas system (Gelegenis et al. 2007; Trine et al. 2004). An active inoculum from a mesophilic biogas agricultural plant in Puglia, Italy was used. The inoculum was taken from an

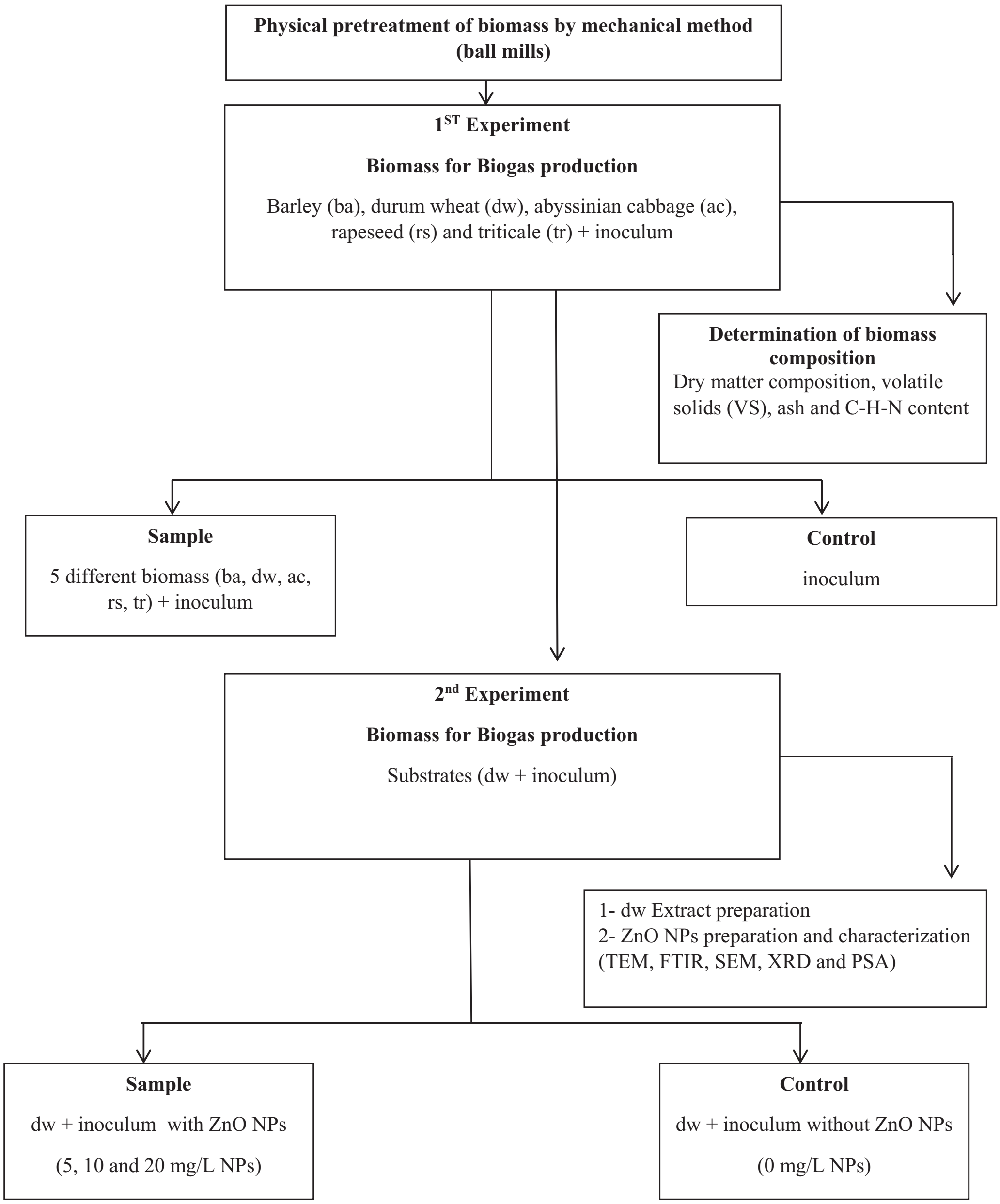

Figure 1. Flow chart of the experimental procedure for chemical and green ZnO NPs.

active anaerobic digester that is digesting complex organic matter and at steady-state of the sampling time. The inoculum was used on the same day of its sampling. Each test was performed with 1 g TS of selected biomass (dried weight) and 20 g of inoculum (wet weight) with a concentration of 8.5% TS, and homogenized by mixing for 15 min.

The cultivation of barley (*Hordeum vulgare L.*), durum wheat (*Triticum turgidum subsp. durum Desf.*), Abyssinian cabbage (*Brassica carinata A.Braun*), rapeseed (*Brassica napus L. var. oleifera D.C.*), and triticale (*Triticale hexaploid Lart.*) was set up in a field located at the experimental farm in Gravina in Puglia located in the central west of the Puglia region (40°49′14″N, 16°25′24″E), Italy an altitude of 385 m above sea level (m.a.s.l.), in fall 2017.

All of the biomass samples were harvested in the spring of 2018 and were ground and sieved to obtain a particle size of 0.38 mm.

Determination of biomass composition

Standard methods (Baird et al. 2012) were applied for total solids (TS) measurement and

Volatile solids (VS), ash content and measurement of C, H, and N were analyzed using the elemental analyzer (Model CHN628). The samples measurements were carried out depending on the complete and instantaneous oxidation method (Friis et al. 1998) with their transformation from organic substrates to gaseous products. The theoretical organic carbon (TOC) was estimated according to the following equation (Cueto et al. 2011):

$$\text{TOC}\ \% = \text{TS}\%/1.724 \qquad (1)$$

Experimental set-up

Laboratory experiments were performed in identical cylindrical syringes digesters as reactors (Gelegenis et al. 2007; Nielfa et al. 2015; Trine et al. 2004). Each reactor is 22 cm in height and 4 cm in diameter with an effective capacity of 100 mL. The syringe is inverted straight into the lid of the reactor. The overpressure inside the reactor pushes the piston until there is a balanced in the pressure buildup to atmospheric pressure (Remigi and Buckley 2006). The volume of biogas can be read off the syringe. The gas was collected with a plastic syringe equipped with a three-way valve and injected back into the waste. The liquid content of each digester has been heated by incubation, monitored by a metallic thermometer located at the mid-depth and adjusted to 37 °C by a thermostat. During the inoculum stirring, 1 L of inoculum was transferred to all reactors (the reactors were placed on a scale).

The influence of different concentrations of ZnO NPs on biogas production was examined by conducting a series of laboratory experiments. The experiments were carried out using 100 mL biodigesters syringes, in batch operation mode. Chemical and green ZnO NPs were synthesized from durum wheat extract and used to study their effects on biogas production compared to the same samples without ZnO NPs. Different doses of ZnO NPs were utilized; 5, 10, and 20 mg L^{-1}, these doses were selected based on previous research. A suspension of ZnO NPs was prepared with sterile Milli-Q water at a concentration of 1000 mg/L. From this solution, aliquots of specific volume corresponding to the final ZnO NPs concentration of the working solution (5 mg/L, 10 mg/L, and 20 mg/L) were added to each digester containing substrate.

The pH of different substrates was measured using a pH meter (Denver instrument Basic) until the steady-state has been achieved. All of the experiments were triplicated including the blank, which indicated the productivity of the inoculum, to obtain the production of the sole substrate. The significant difference among the experiments was calculated using the *T*-test in Microsoft Excel.

Synthesis of ZnO NPs

Chemical ZnO NPs

A 0.2 M of zinc acetate dihydrate ($Zn(CH_3COO)_2.2H_2O$) was added to 500 mL of distilled water under continuous stirring for 15 min followed by the addition of 0.5 M NaOH dropwise until the pH became 12 and a pale white color was achieved. The solution was stirred for 2 h and the attained pale white precipitate was separated, washed several times with distilled water, followed by ethanol and left for drying at 80 °C under vacuum overnight. The attained powder was calcined at 500 °C for 2.5 h. The pale white powder of ZnO NPs was carefully collected and kept till usage.

Green ZnO NPs

The extract from durum wheat wastes was prepared by washing ten grams of durum wheat powder with double distilled water (DDW), drying at room temperature (28 °C), and grinding with a mortar. The produced powder was added to Erlenmeyer containing 1000 mL of DDW. The final mixture was refluxed at 70–80 °C for 3 h and let it cool at room temperature. The mixture was centrifuged at 6000 rpm for 10 min, and the supernatant was collected and stored at −20 °C for further processing.

A 10 mL of the aqueous extract from durum wheat was added to the Zinc acetate dehydrate and the distilled water, and then followed by the same procedures of the chemical ZnO NPs procedures.

Characterization of structural properties of ZnO NPs

The surface morphology features and homogeneity were characterized using a scanning electron

Table 1. The mean values of the chemical composition for the different biomass samples.

Biomass	TS (%)	Ash (% from TS)	VS (% from TS)	N (%)	C (%)	H (%)	C/N	TOC (%)
Barley	49.23 ± 0.0002	5.21 ± 0.833	94.79 ± 0.0285	1.08 ± 0.204	52.06 ± 0.716	6,39 ± 0.0005	48.27 ± 0.01	54.98 ± 0.749
Durum wheat	43.25 ± 0.001	4.34 ± 0.481	95.66 ± 0.351	1.87 ± 0.001	52.51 ± 0.568	6,67 ± 0.0012	28.12 ± 0.352	55.49 ± 0.968
Abyssinian cabbage	36.52 ± 0.0008	6.09 ± 0.312	93.91 ± 0.0013	1.36 ± 0.615	52.01 ± 0.658	6.35 ± 0.0006	38.26 ± 1.034	54.47 ± 1.093
Rapeseed	36.14 ± 0.001	6.94 ± 1.252	93.06 ± 0.671	1.54 ± 0.613	55.94 ± 1.259	6.70 ± 0.0018	36.23 ± 0.327	53.98 ± 0.001
Triticale	44.52 ± 0.0012	5.58 ± 0.0068	94.42 ± 0.591	0.75 ± 0.161	51.94 ± 0.0191	6.40 ± 0.0017	69.63 ± 1.339	54.77 ± 1.103

TOC: theoretical organic carbon.

microscope (SEM - JEOL JSM 6360LA, Japan). SEM analysis was done with an accelerating voltage of 20 kV at room temperature.

The SEM system equipped with energy-dispersive X-ray spectroscopy (EDX) detector, which is used to determine the substances elemental composition, is used in this study to ensure the purity of the synthesized ZnO NPs.

The nanostructure of ZnO NPs was investigated by transmission electron microscope (JEOL Ltd., Tokyo, Japan). The samples were dispersed in EtOH and then treated ultrasonically to disperse the individual particles over the gold grid.

The structure and the functional groups of the prepared ZnO NPs were confirmed by using (IRAffinity-1SFTIR spectrometer Shimadzu, Japan) after their preparation in the form of KBr pellets following the procedures described by (Soliman et al. 2018).

X-ray diffractograms for ZnO NPs were obtained using a (Shimadzu XRD-7000 diffractometer, Japan) operating at 40 kV, 30 mA with Cu Kα, Ni-filtered radiation ($\lambda = 1.5418$ Å) and equipped with the computer application software (DP-D1, Shimadzu Co. Ltd.). The specimen was placed in the sample holder and scanned at 2θ from 5 to 80° at a rate of 2°/min to determine the ZnO NPs crystallographic structure. The particle size analyzer (PSA) model: N5 submicron, to measure the size and distribution of ZnO, was also applied. The mean pore diameter and specific surface area [BET (Brunauer–Emmett–Teller)] were measured by using (BELSORP - Mini II, BEL Japan, Inc.).

Results and discussion

Characterization of different agricultural crops

Total solids, C, N content and C/N ratio

The biomass TS content varies from about 36 to 50% as shown in Table 1 with a mean value of 41.88%. All biomass samples have no S content. C/N ratio varies from about 28 to 69 with an average of 44.1, Table 1. The range of 20-30 C/N is specified as the optimal range in a previous study (Bardiya and Gaur 1997). However, other studies (Kivaisi and Mtila 1997; Nyns 1986) reported that the optimal C/N ratio is 16–19 for methanogenic performance when poorly degradable compounds such as lignin are taken into account (Mshandete et al. 2004). From the C/N ratio results, it is clear that the highest biogas yield was produced by utilizing durum wheat that has a C/N ratio of 28.12 which falls in the optimal range as suggested by literature (20–30). While the lowest biogas yield was obtained from the triticale biomass that has a C/N ratio of 69.63.

Characterization of ZnO NPs

Scanning electron microscopy (SEM)

The surface profile of ZnO NPs was taken at high magnification (10kX) as shown in Figure 2(a,b). The images proved that the synthesized ZnO particles are on the nanoscale. For the chemically synthesized ZnO, the external surface is convex and concave flower-like particles with many apertures distributed along the ZnO surface. While in the case of the green synthesized ZnO, the surface is semi-flat with rod-like particles and low apertures, which may lead to increase the contacting surface and therefore, increase the reactivity.

Energy-dispersive X-ray spectroscopy (EDX)

Zn and O energy peaks were observed using EDX spectra to determine the elemental contents of typical points on the chemical and green synthesized ZnO NPs surface. Table 2 showed that Zn contents on the chemical and green surfaces are 85.85 and 88.55 mass%, respectively, which indicates the higher purity of the green ZnO

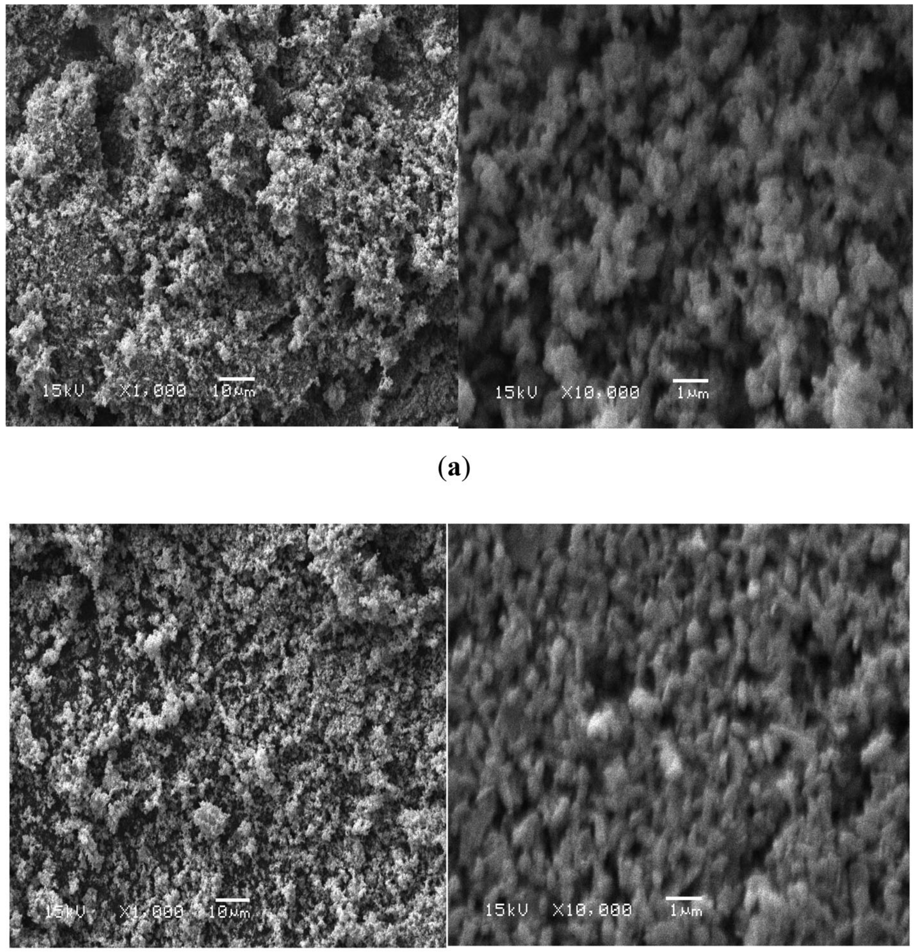

Figure 2. SEM images of (a) chemical and (b) (Wheat) Green synthesized ZnO NPs.

Table 2. EDX spectra to determine the elemental contents of typical points on the chemical and green synthesized ZnO NPs surface.

	Elements content		
Materials	O	Na	Zn
Chemical ZnO	5.2 ± 0.2	9.13 ± 0.4	85.85 ± 3.3
Green ZnO	4.18 ± 0.8	7.27 ± 0.5	88.55 ± 2.2

NPs. The sole impurity that existed in both chemical and green ZnO NPs is Na which leads to lowering the net ZnO content.

Transmission electron microscope (TEM)

The nanoparticles morphology and distribution are characterized by a transmission electron microscope (TEM). The green synthesized ZnO NPs are smaller and well-defined particles with homogeneous spreading than the chemical synthesized ZnO NPs which are larger and more compact. The chemical synthesized ZnO NPs ranged between 9 and 40 nm with an average size of 24.5 nm, while the green synthesized ZnO NPs ranged between 5 and 28 nm with an average size of 16.5 nm as presented in Figure 3(a,b).

Fourier transform infrared spectra (FTIR). The structure of chemically and green synthesized ZnO NPs is confirmed by IR spectroscopy. As shown in Figure 4, the IR pattern of the two synthesized ZnO NPs is very close and near to be identical. The peak at 897 cm^{-1} confirms the presence of Zn-O stretching vibration (Kansal et al. 2013). From the literature, the peak at 1628 cm^{-1} is attributed to O-H stretching vibration of H-O-H (Hassan et al. 2015; Kataria and Garg 2017). The asymmetric and symmetric stretching vibration peak indicating presence of CH_2 and/or CH_3 was observed at 2933 cm^{-1}. The broad peak around 3441 cm^{-1} is assigned for the OH stretching vibrations of chemisorbed and/or physisorbed water (Ali et al. 2015, 2019; Soliman

(a)

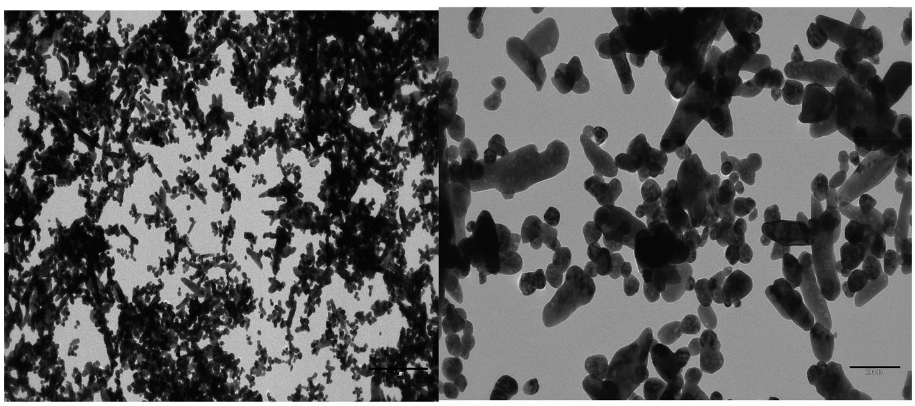

(b)

Figure 3. TEM images of (a) chemical and (b) (Wheat) Green synthesized ZnO NPs.

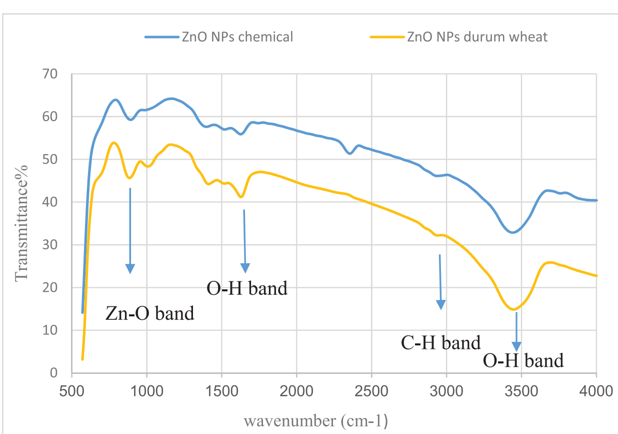

Figure 4. The FTIR Spectrum of chemical and green synthesized ZnO NPs.

et al. 2018). Ali et al. (2015) reported that the presence of –OH bonds on the surface of solid chemicals enhances its catalytic activity.

X-ray diffractograms (XRD)

The XRD pattern of chemically and green synthesized ZnO NPs is shown in Figure 5. The diffraction peaks at $2\theta = 31.9$, 34.3, 37, 47.5, 56.5, 63.2, 68, and 69.2° is similar to the diffraction plane (100), (002), (101), (102), (110), (103), (200), (112), and (201) respectively. The obtained peaks demonstrate that the powder is highly crystalline and in good agreement with the hexagonal structure, with the absence of peaks from other ZnO phases. Matching the diffraction peaks of the two synthesized ZnO NPs with the standard one confirmed that the synthesized particles are composed of pure ZnO (Hassaan et al. 2019; Wang et al. 2013).

The particle size analyzer (PSA)

Figure 6(a) shows the particle size distribution determined by PSA for chemical ZnO NPs. The chemical ZnO NPs have non-uniform particle size as a result of detecting ZnO particles in the range from 6 to 8 nm which were determined using a 10.9° test angle and another range of particle size from about 200 to 250 nm which were determined using 90° test angle. While in the

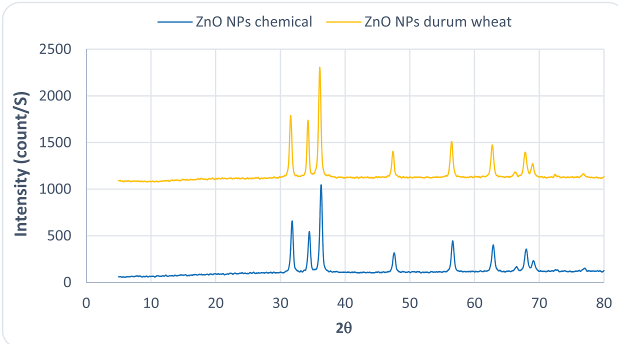

Figure 5. The XRD patterns of chemical and green synthesized ZnO NPs.

case of green ZnO, all particles were uniform and homogeneous as they were all detected by the10.9° test angle and all the particles in the range of 3 nm while by using the 90° test angle the particles were in the range of 95 nm as shown in Figure 6(b). The uniformity and homogeneity of the green ZnO NPs may affect biogas production positively.

BET surface area and porosity

Table 3 demonstrates the results of the surface area of ZnO NPs which ranged from 12.9 to

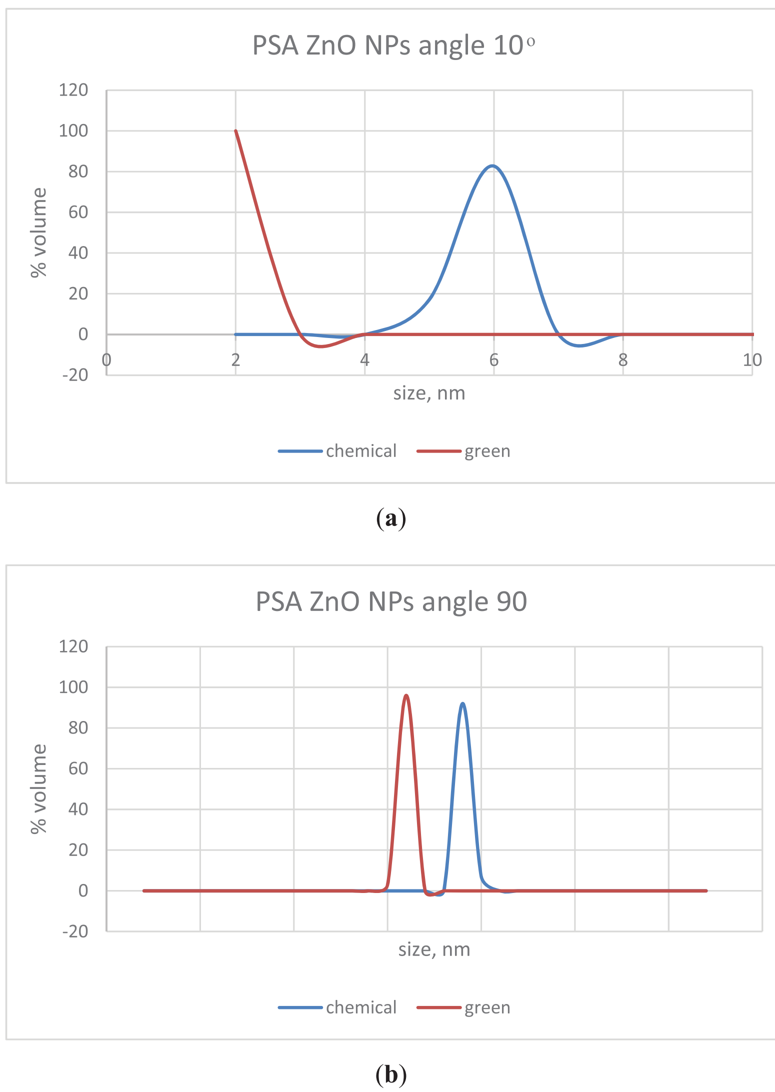

Figure 6. PSA images of (a) chemical and (b) (Wheat) Green synthesized ZnO NPs.

Table 3. BET Surface area and porosity of chemical and green ZnO NPs.

Total pore volume (cm^3/g)	Mean pore diameter (nm)	BET surface area (m^2/g)	Material
0.02789	8.64	12.90	Chemical ZnO NPs
0.03436	9.63	14.26	Green ZnO NPs

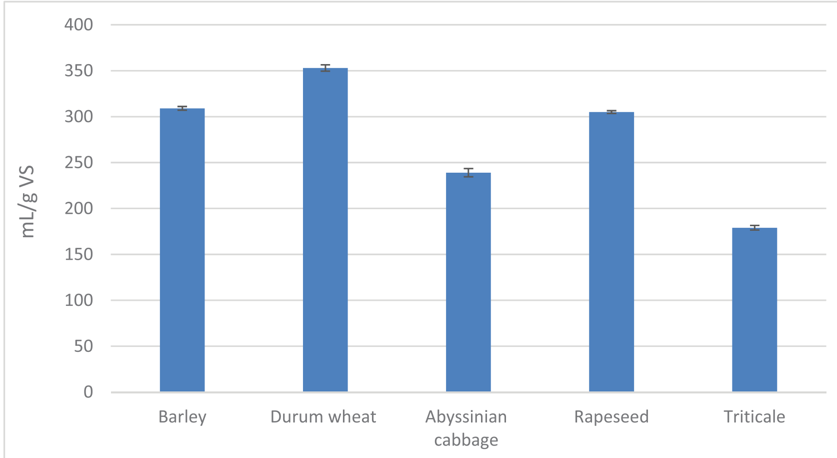

Figure 7. The average values of the net volume of biogas mL/g VS (1st experiment).

14.26 m^2/g and pore volume from 0.03436 to 0.02789 cm^3/g for both chemical and green ZnO NPs respectively. The surface area and pore volume of chemical Zn NPs are lower than the green Zn NPs which may be due to the high annealing temperature which may be lead to collapse the pores and agglomerate the nanoparticles that lead to reduce the specific surface area and the pore volume (Ismail et al. 2018; Sivakami et al. 2016). These results also agree with Ismail et al. who obtained a notable reduction in the ZnO NPs surface area from 25.36 to 8.78 m^2/g by raising the temperature from 275 °C to 650 °C. Moreover, these results are compatible with the rod-like particle morphology that is observed by SEM analysis and the smaller particle size of the green ZnO NPs than the chemical ZnO NPs which are detected by PSA and TEM analysis that are considered as the direct reasons for the higher surface area of green ZnO NPs than chemical ZnO NPs.

Monitoring of biogas production

Biogas production from the first Exp

The results were determined during a period of 25 days. The first-week biogas production yield is higher than the next weeks, these results agree with the literature (Bussemaker and Zhang 2013; Cundr and Haladová 2014). By comparing the different biomasses for direct biogas production, it was found that durum wheat biomass produces the highest biogas yield of 353 mL/g VS, as shown in Figure 7. The high significant durum wheat biogas production yield of 353 mL/g VS ($p < 0.05$), could be obtained in a low C/N ratio (28.12) which is included through the optimum range suggested by previous work (Bardiya and Gaur 1997). While the lowest biogas yield was obtained from utilizing the triticale biomass with an average yield of 179 mL/g VS, Figure 7. The low digestibility of triticale may be due to the high content of lignin and the existence of other barely digestible materials in the substrate or/and could be due to the high C/N ratio which reaches 69.63 as shown in Table 1. From Table 1 and Figure 7, we can notice the higher biogas yield of rapeseed and this may be attributed to the C/N ratio (36.23), it is even slightly higher than the optimum range suggested by previous studies (20–30), (Bardiya and Gaur 1997).

The effect of ZnO NPs on biogas production from the second Exp

The experimental results of biogas production yield were collected during a period of 25 days and plotted in Figure 8(a,b). The high production results during the first week are in agreement with other biogas literature (Hassaan et al. 2018; Popescu and Mastorakis 2010). The mean biogas production yield was enhanced by treating the durum wheat with 5 and 10 mg L^{-1} ZnO NPs and compared with the biogas production yield from substrates without using both chemical and green ZnO NPs as shown in Figure 8. The low doses of both chemical and green ZnO NPs (5 mg L^{-1}) have a significantly positive impact on biogas production with ($p < 0.05$). Using 10 mg

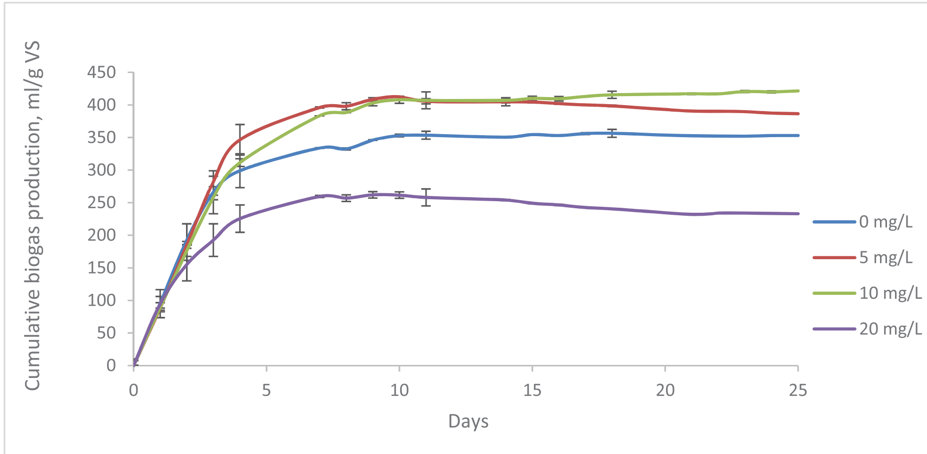

(a)

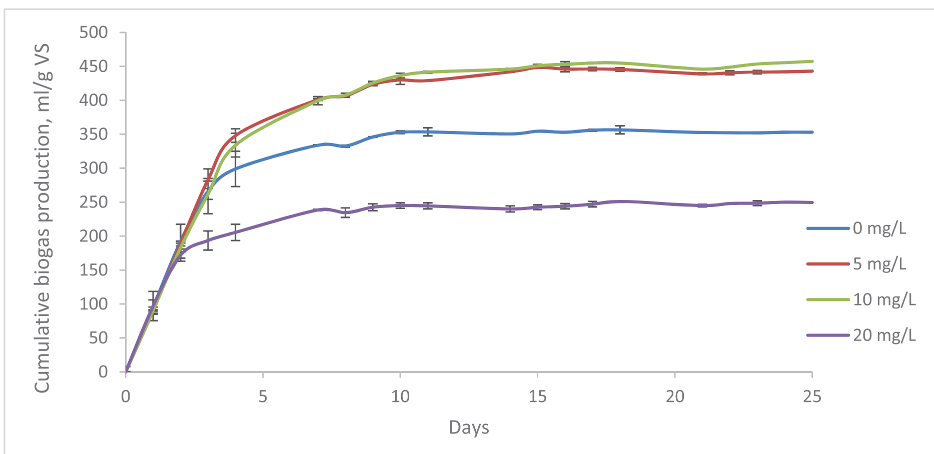

(b)

Figure 8. The mean cumulative net biogas production using (a) chemical and (b) green ZnO NPs.

L^{-1} ZnO NPs produces higher biogas yield than 5 mg L^{-1}. While utilizing 20 mg L^{-1} of both chemical and green ZnO NPs has inhibitory effects on the biogas production. Hence, the optimum ZnO NPs dose of 10 mg L^{-1} can be considered as 10 mg L^{-1}. The biogas production tests were terminated when the biogas daily production was less than 1% of the whole production as noticed in Figure 9(a,b). This research analyzes the positive impact of both green and chemical synthesized ZnO NPs on the biogas production from durum wheat, which is in agreement with previous studies (Amirante et al. 2018) who used only green ZnO NPs and with another study (Abdelsalam et al. 2017) who used only chemical Fe NPs. It is also worth to mention that, the biogas yield of this study is higher than another study implemented by (Hassaan et al. 2018) who studies the impact of both chemical and green ZnO NPs on the biogas yield from wheat silage.

The initial anaerobic process that produced a high biogas yield in the first week is followed by inactivity which is possibly due to the methanogens experiencing a metamorphic growth activity (Bal and Dhagat 2001; Elijah et al. 2009). These results generally agree with the fact that at the primary stages of the total process of biogas production, acid-forming bacteria produce VFA resulting in reducing pH and preventing the growth of methanogenic bacteria (Bussemaker and Zhang 2013). The low pH values deactivated the microorganisms accountable for biogas

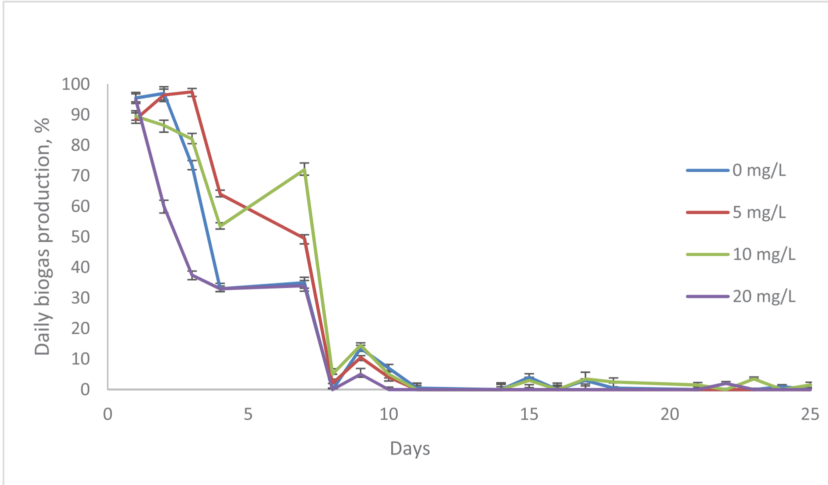

(a)

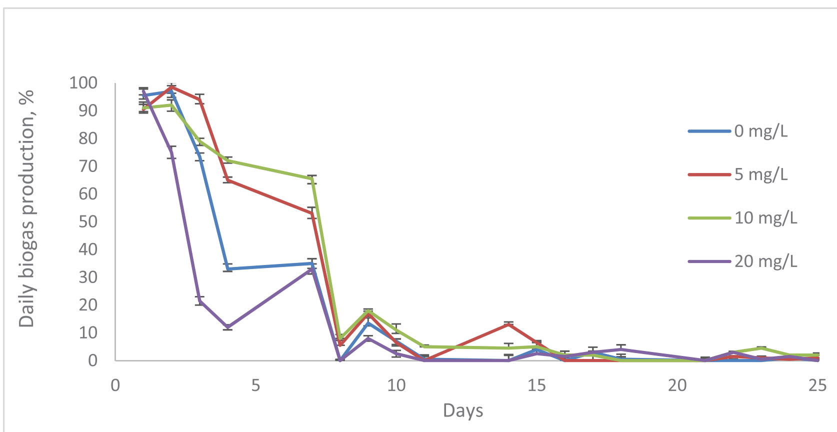

(b)

Figure 9. Mean rate percentage of daily biogas production using (a) chemical and (b) green ZnO NPs.

generation (Bal and Dhagat 2001; Cuzin et al. 1992). The pH of the substrate (wheat with inoculum) is reduced from 8.03 to 6.5 for wheat during the first week.

Previous researches showed that using NPs can increase the biogas production yield due to the ability of specific NPs to improve the biological activity through long-term exposure by releasing the metal ions from the metal NPs which plays an important role in microbial communities included in biological treatment processes (Ni et al. 2013; Wang et al. 2016). Moreover, direct interspecies electron transfer by metal NPs can play an important role in facilitating the methanogenesis process during the AD process (Wang et al. 2016). It has been reported that the reduced electron carriers can regenerate into H_2 which serve as an electron donor and combine with CO_2 to produce CH_4 (Cruz Viggi et al. 2014; Summers et al. 2010). Additionally, Ganzoury and Allam (2015) stated that the high surface area of the NPs has a positive effect on the AD process. In this study, the surface area of ZnO NPs showed that green ZnO NPs has a higher surface area more than chemical ZnO NPs which may lead to enhance biogas production Table 3. Furthermore, NPs have a great potential on the enzymatic activities of the methanogenesis bacteria rather than affecting the biomass itself. The combination of using NPs and other pretreatment techniques such as sonication and ozonation that affect the biomass may increase the biogas productivity.

Previous studies stated that the lethal metal ions released from the dissolution of NPs were mainly liable for their toxicity to definite living creatures (Brunner et al. 2006; Franklin et al. 2007; Wang et al. 2016; Xia et al. 2008). This mechanism might clarify the toxicity of soluble NPs, such as ZnO NPs (Mu and Chen 2011). Other literature has reported ZnO NPs were powerfully lethal due to their dissolution (Franklin et al. 2007). However, in the present study, the improvement of biogas production was observed at a lower doses of ZnO NPs (i.e., 5 mg/L), while biogas production was inhibited by the higher dose of ZnO NPs (i.e., 20 mg/L).

Scientists have discovered that many NPs may be adsorbed onto and/or reacted with cell membranes and can then disrupt them. Zhang et al. (2007) detected that ZnO NPs injured the bacterial cell membrane. Most scientists trust that the metal ions released from NPs play a significant role in microorganism populations that are included in biological treatment processes (Wang et al. 2016). Some scientists found that higher concentrations of metal ions released from NPs inhibited these microorganism populations during the sewage sludge treatment process (Wang et al. 2016). Xia et al. revealed that the toxicity of ZnO NPs to the lysosomes and mitochondria of microorganism communities was due to the damage of intracellular Zn homeostasis. This work agrees with the previous studies in some points such as; the higher concentrations of ZnO NPs can be toxic and inhibits bacterial growth while the lower doses of ZnO NPs can enhance biogas production. Also, this study is the first study that investigates the effect of green synthesis of ZnO NPs on biogas production from durum wheat which resulted in a higher biogas yield in comparison with chemical ZnO NPs that investigated only in the previous publications. The results proved that using ZnO NPs can not only increase biogas production yield but can also decrease the number of days required to reach peak biogas production (Figure 8). Moreover, as confirmed from PSA and TEM analysis: the green synthesized ZnO NPs are smaller and well-defined particles with homogeneous spreading than the chemical synthesized ZnO NPs which are larger and more compact. These smaller green synthesized ZnO NPs have a larger surface area with a positive impact on biogas production which is the reason to produce a higher yield than in chemical ZnO NPs. The literature survey shows that using plants offers important advantages over other biological systems. The plants are easily available and safe to handle and the nanoparticles synthesized by plants extracts are more stable (Iravani 2011). Moreover, the nanoparticles prepared by green methods are more stable and have low toxicity in comparison with the nanoparticles prepared by chemical methods which may not be suitable for biological activities such as in biogas processes due to its toxicity. In this work, chemical ZnO NPs have been synthesized using distilled water only instead of using ethanol or other chemical solvents for the synthesis method which may be the reason for the biogas production enhancement using chemical ZnO NPs even it still lower than the green synthesized ZnO NPs.

Conclusions

From the aforementioned results, it can be concluded that:

1. Successfully manufacturing of green ZnO NPs using durum wheat extract which contains phytochemicals components acting as capping and stabilizing agents.
2. The durum wheat biomass has the highest biogas production yield in comparison with the other four tested biomass crops in the first exp with biogas production yield of 353 mL/g VS.
3. In the second exp, the improvement of the biogas production was attained by adding 5 and 10 mg/L of ZnO NPs. In particular, the biogas production yield is increased from 353 mL/g VS using the durum wheat biomass without ZnO NPs to 422 and 457 mL/g VS using 10 mg/L of chemical and green ZnO NPs respectively.
4. On the other side, higher ZnO NPs loading (20 mg/L) has an inhibitory effect on methanogenesis bacteria. Green synthesized ZnO NPs provided a higher biogas production yield than chemical synthesized ZnO NPs by 13% and 8% for 5 and 10 mg/L respectively. Hence, it can be confirmed that, the treating of wheat with green synthesized ZnO NPs is a promising

technology to increase the biogas production yield.

ORCID

Mohamed A. Hassaan http://orcid.org/0000-0002-8513-5304

References

Abdelsalam E, Samer M, Attia YA, Abdel-Hadi MA, Hassan HE, Badr Y. 2017. Influence of zero valent iron nanoparticles and magnetic iron oxide nanoparticles on biogas and methane production from anaerobic digestion of manure. Energ J. 120:842–853. doi:10.1016/j.energy.2016.11.137

Ali RM, Abd El Latif MM, Farag HA. 2015. Preparation and characterization of $CaSO_4$–SiO_2–CaO/SO_4^{2-} composite for biodiesel. Am J Appl Chem. 3:38–45.

Ali R, El Katory M, Hassaan M, Amer K, El Geiheini A. 2019. Highly crystalline heterogeneous catalyst synthesis from industrial waste for sustainable biodiesel production. Egypt J Chem. doi:10.21608/ejchem.2019.15471.1943

Amirante R, Demastro G, Distaso E, Hassaan MA, Mormando A, Pantaleo AM, Tamburrano P, Tedone L, Clodoveo ML. 2018. Effects of ultrasound and green synthesis ZnO nanoparticles on biogas production from Olive Pomace. Energy Procedia. 148:940–947. doi:10.1016/j.egypro.2018.08.091

Baird RB, Bridgewater L, Clesceri LS, Eaton AD, Rice EW, editors. 2012. Standard methods for the examination of water and wastewater. Washington, DC: American Public Health Association.

Bal AS, Dhagat NN. 2001. Up flow anaerobic sludge blanket reactor. Indian J Environ Health. 43(2):1–82.

Bardiya N, Gaur AC. 1997. Effects of carbon and nitrogen ratio on rice straw bio-methanation. J Rural Energy. 4:1–16.

Borjesson P, Berglund M. 2006. Environmental systems analysis of biogas system Part I: Fuelcycle emissions. Biomass Bioenerg. 30:469–485. doi:10.1016/j.biombioe.2005.11.014

Brunner TJ, Wick P, Manser P, Spohn P, Grass RN, Limbach LK, Bruinink A, Stark WJ. 2006. In vitro cytotoxicity of oxide nanoparticles: comparison to asbestos, silica, and the effect of particle solubility. Environ Sci Technol. 40(14):4374–4381. doi:10.1021/es052069i

Bussemaker MJ, Zhang D. 2013. Effect of ultrasound on lignocellulosic biomass as a pretreatment for biorefinery and biofuel applications. Ind Eng Chem Res. 52(10):3563–3580. doi:10.1021/ie3022785

Cruz Viggi C, Rossetti S, Fazi S, Paiano P, Majone M, Aulenta F. 2014. Magnetite particles triggering a faster and more robust syntrophic pathway of methanogenic propionate degradation. Environ Sci Technol. 48(13):7536–7543. doi:10.1021/es5016789

Cueto MJ, Fernandez C, Omez X, Moran A. 2011. Anaerobic co-digestion of swine manure with energy crop residues. Biotechnol Bioprocess Eng. 16:1044–1052.

Cundr O, Haladová D. 2014. Biogas yield from Anaerobic batch co-digestion of rice straw and zebu dung. SAB. 45:98–103. doi:10.7160/sab.2014.450204

Cuzin N, Farinet JL, Segretain C, Labat M. 1992. Methanogenic fermentation of cassava peel using a pilot plug flow digester. Bioresour Technol. 41(3):259–264. doi:10.1016/0960-8524(92)90011-L

Elijah T, Ibifuro A, Yahaya SM. 2009. The study of cow dung as co-substrate with rice husk in biogas production. Scientific Res Essay. 9:861–866.

Franklin NM, Rogers NJ, Apte SC, Batley GE, Gadd GE, Casey PS. 2007. Comparative toxicity of nanoparticulate ZnO, bulk ZnO, and ZnCl2 to a freshwater microalga (Pseudokirchneriella subcapitata): the importance of particle solubility. Environ Sci Technol. 41(24):8484–8490. doi:10.1021/es071445r

Friis J, Holm C, Halling-Sørensen B. 1998. Evaluation of elemental composition of algal biomass as toxical endpoint. Chemosphere. 13:2665–2676. doi:10.1016/S0045-6535(98)00153-2

Ganzoury MA, Allam NK. 2015. Impact of nanotechnology on biogas production: a mini-review. Renew Sust Energ Rev. 50:1392–1404. doi:10.1016/j.rser.2015.05.073

Gelegenis J, Georgakakis D, Angelidaki I, Mavris V. 2007. Optimization of biogas production by co-digesting whey with diluted poultry manure. Renew Energ. 32(13):2147–2160. doi:10.1016/j.renene.2006.11.015

Gustavsson J, Svensson BH, Karlsson A. 2011. The feasibility of trace element supplementation for stable operation of wheat sillage-fed biogas tank reactors. Water Sci Technol. 64(2):320–325. doi:10.2166/wst.2011.633

Hassaan M, El Katory M, Ali R, El Nemr A. 2019. Photocatalytic degradation of reactive black 5 using Photo-Fenton and ZnO nanoparticles under UV irradiation. Egypt J Chem. 0(0):0–0. doi:10.21608/ejchem.2019.15799.1955

Hassaan MA, Pantaleo A, Tedone L, Demastro G. 2018. Biogas production from silage flour wheat influenced by chemical and green synthesized ZnO nanoparticles. In: Proceedings of XLVII Conference of Italian Society for Agronomy; 2018 Sep 12–14; Marsala, Italy.

Hassan SSM, El Azab WIM, Ali HR, Mansour MSM. 2015. Green synthesis and characterization of ZnO nanoparticles for photocatalytic degradation of anthracene. Adv Nat Sci Nanosci Nanotechnol. 6:1–12.

Iravani S. 2011. Green synthesis of metal nanoparticles using plants. Green Chem. 13(10):2638–2650. doi:10.1039/c1gc15386b

Ismail MA, Taha KK, Modwi A, Khezami L. 2018. ZnO nanoparticles: surface and X-ray profile analysis. J Ovonic Res. 14(5):381–393.

Kamel DA, Farag HA, Amin NK, Zatout AA, Ali RM. 2018. Smart utilization of Jatropha (Jatropha curcas Linnaeus) seeds for biodiesel production: Optimization and mechanism. Ind Crops Prod. 111:407–413. doi:10.1016/j.indcrop.2017.10.029

Kansal SK, Lamba R, Mehta SK, Umar A. 2013. Photocatalytic degradation of Alizarin Red S using simply synthesized ZnO nanoparticles. Mater Lett. 106:385–389. doi:10.1016/j.matlet.2013.05.074

Kataria N, Garg VK. 2017. Removal of Congo red and Brilliant green dye from aqueous solution using flower shaped ZnO nanoparticles. J Environ Chem Eng. 5(6): 5420–5428. doi:10.1016/j.jece.2017.10.035

Kivaisi AK, Mtila M. 1997. Production of biogas from water hyacinth (Eichhorniacrassipes) in a two stage bioreactor. World J Microbiol Biotechnol. 14(1):125–131.

Mshandete A, Kivaisi A, Rubindamayugi M, Mattiasson B. 2004. Anaerobic batch co-digestion of sisal pulp and fish wastes. Bioresour Technol. 95(1):19–24. doi:10.1016/j.biortech.2004.01.011

Mu H, Chen Y. 2011. Long-term effect of ZnO nanoparticles on waste activated sludge anaerobic digestion. Water Res. 45(17):5612–5620. doi:10.1016/j.watres.2011.08.022

Mu H, Chen Y, Xiao N. 2011. Effects of metal oxide nanoparticles (TiO_2, Al_2O_3, SiO_2 and ZnO) on waste activated sludge anaerobic digestion. Bioresour Technol. 102(22): 10305–10311. doi:10.1016/j.biortech.2011.08.100

Ni SQ, Ni J, Yang N, Wang J. 2013. Effect of magnetic nanoparticles on the performance of activated sludge treatment system. Bioresour Technol. 143:555–561. doi:10.1016/j.biortech.2013.06.041

Nielfa A, Cano R, Fdz-Polanco M. 2015. Theoretical methane production generated by the co-digestion of organic fraction municipal solid waste and biological sludge. Biotechnol Rep. 5:14–21. doi:10.1016/j.btre.2014.10.005

Nyns EJ. 1986. Biomethanation processes. Weinheim, Berlin: Wiley-VCH. p. 207–267.

Popescu MC, Mastorakis N. 2010. Aspects regarding the use of renewable energy in EU Countries. WSEAS Trans. 4: 265–275.

Qiang H, Lang DL, Li YY. 2012. High-solid mesophilic methane fermentation of food waste with an emphasis on Iron, Cobalt, and Nickel requirements. Bioresour Technol. 103(1):21–27. doi:10.1016/j.biortech.2011.09.036

Remigi EU, Buckley CA. 2006. Co-digestion of high strength/toxic organic effluents in anaerobic digesters at Wastewater Treatment Works; Water Research Commission: Pretoria, South Africa.

Risco LMK, Orupold K, Dubourguier HC. 2011. Particle-size effect of CuO and ZnO on biogas and methaneproduction during anaerobic digestion. J Hazard Mater. 189:603–608. doi:10.1016/j.jhazmat.2011.02.085

Schmidt T, Pröter J, Scholwin F, Nelles M. 2013. Anaerobic digestion of grain stillage at high organic loading rates in three different reactor systems. Biomass Bioenerg. 55: 285–290. doi:10.1016/j.biombioe.2013.02.010

Sivakami R, Dhanuskodi S, Karvembu R. 2016. Estimation of lattice strain in nanocrystalline RuO2 by Williamson–Hall and size–strain plot methods. Spectrochim Acta Part A: Mol Biomol Spectrosc. 152: 43–50. doi:10.1016/j.saa.2015.07.008

Soliman EA, Elkatory MR, Hashem AI, Ibrahim HS. 2018. Synthesis and performance of maleic anhydride copolymers with alkyl linoleate or tetra-esters as pour point depressants for waxy crude oil. Fuel. 211:535–547. doi:10.1016/j.fuel.2017.09.038

Summers ZM, Fogarty HE, Leang C, Franks AE, Malvankar NS, Lovley DR. 2010. Direct exchange of electrons within aggregates of an evolved syntrophiccoculture of anaerobic bacteria. Science. 330(6009):1413–1415. doi:10.1126/science.1196526

Takashima M, Speece RE, Parkin GF. 2009. Mineral requirements for methane fermentation. Crit Rev Environ Control. 19(5):465–479. doi:10.1080/10643389009388378

Trine LH, Jens ES, Irini A, Emilia MCJ, Hans M, Thomas HC. 2004. Method for determination of methane potentials of solid organic waste. Waste Manage. 24:393–400.

Wang T, Zhang D, Dai L, Chen Y, Dai X. 2016. Effects of metal nanoparticles on methane production from waste-activated sludge and microorganism community shift in anaerobic granular sludge. Sci Rep. 6:1–10. doi:10.1038/srep25857

Wang X, Cai W, Liu S, Wang G, Wu Z, Zhao H. 2013. ZnO hollow microspheres with exposed porous nanosheets surface: Structurally enhanced adsorption towards heavy metal ions. Colloids Surf A Physicochem Eng Asp. 422:199–205. doi:10.1016/j.colsurfa.2013.01.031

Xia T, Kovochich M, Liong M, Madler L, Gilbert B, Shi H, Yeh JI, Zink JI, Nel AE. 2008. Comparison of the mechanism of toxicity of zinc oxide and cerium oxide nanoparticles based on dissolution and oxidative stress properties. ACS Nano. 2(10):2121–2134. doi:10.1021/nn800511k

Zhang L, Jiang Y, Ding Y, Povey M, York D. 2007. Investigation into the antibacterial behaviour of suspensions of ZnO nanoparticles (ZnO nanofluids. J Nanopart Res. 9(3):479–489.